

Rolling Texture Development in Aluminum-Zinc Solid Solutions

B.J. Diak, B. Merkle, O. Gopkalo

Mechanical and Materials Engineering, Queen's University, Kingston, Ontario, Canada, K7L3N6

diak@queensu.ca

Abstract. Rolling textures in face-centered cubic polycrystalline metals tend to transform from so-called pure metal to alloy textures with increasing stacking fault energy, so deformation texture correlates directly to stacking fault energy. As a 30th anniversary tribute to the classic copper-brass study by Hirsch and Lücke [1988], we recast the problem for binary aluminium alloys with 1, 10, 34 and 62wt.%Zn. Zinc (Zn) has a very high solid solubility in Al of up to 65at.% at 381°C, but at lower temperatures the Zn solid solution is unstable and can precipitate out or decompose spinodally. Current understanding is that Zn has no effect on the stacking fault energy of aluminum, so a priori, rolling of different Al-xZn alloys should result in no variation in deformation texture. Cast ingots were solutionized and promptly rolled 75 and 90% by multiple passes. X-ray texture pole figures were measured at the mid-plane of the rolled sheet, and the texture components calculated from the crystallographic orientation distribution function. Results show a decrease in $\{112\}\langle 11-1 \rangle$ and increase in $\{011\}\langle 21-1 \rangle$ with Zn content but uncorrelated changes in $\{123\}\langle 63-4 \rangle$ components. Bird's eye - like microstructural features observed in the high Zn containing alloys at 90% reduction were $\{011\}\langle 21-1 \rangle$ and resemble those observed by other researchers in severely rolled brass, Al-4.5Mg and 316L.

1. Introduction

Aluminum (Al) has a relatively high stacking fault energy compared to other face-centered cubic (f.c.c.) crystalline elements, and so its deformation is often characterized by greater potential for cross-slip and recovery at higher temperatures and organization of a more cellular work-hardened dislocation structure. It has been observed that the rolling textures in face-centered cubic polycrystalline metals tend to transform from so-called pure metal to alloy textures with decreasing stacking fault energy, so deformation texture correlates with stacking fault energy. In one of the first quantitative studies of deformation textures Hirsch and Lücke [1] used the calculated crystallographic orientation distribution function to quantify the role of rolling reduction and Zn content on the texture evolution of copper and α -brass. As a 30th anniversary tribute to this study, we recast the problem for binary Al alloys with 1, 10, 30 and 60wt.%zinc. Zinc (Zn) has a very high solid solubility in Al of up to 83wt.% (65at.%) at 381°C, but at lower temperatures the Zn solid solution is unstable and can precipitate out or decompose spinodally [2-5]. It is mutedly accepted that Zn has no effect on the stacking fault energy of aluminum [5, 6], so a priori, rolling of solutionized Al-xZn alloys should result in no variation in deformation texture due to slip compared to pure Al.

The objective of the present work is to study the rolling texture development in Al-xZn alloys aux Hirsch and Lücke [1] to indirectly test if Zn modifies the intrinsic stacking fault energy of aluminum.



2. Experimental Procedure

2.1 Alloy preparation

Five aluminum alloys with target compositions of 0, 1, 10, 30 and 60wt.%Zn were prepared from 99.99 or 99.97wt.%Al, and 99.99wt.%Zn starting materials. For each melt composition Al was placed in a refractory crucible coated with red mud and gas fired to 800°C after which TiB₂ wafer was added for grain refining, followed by addition of the Zn and stirred with a graphite rod. To reduce Zn loss to vaporization, excess Zn was added according to past practice and the temperature lowered to about 70°C above the liquidus for as superheat for each composition. Dross was skimmed from the melt surface before gravity pouring into a graphite-coated steel book mold at the temperatures listed in Table 1 and air cooled with no chill. The ingots were scalped, wrapped in aluminum foil and then homogenized at 428°C for 96 hours in a salt bath and water quenched to room temperature. Chemical analysis of the homogenized castings listed in Table 2 indicates compositions close to the targets and are subsequently identified by these chemistries. The differences in Fe and Si content between the pure Al and Al-1wt.%Zn, and other alloys is due to the use of a 99.99 Al master alloy for the former two.

Table 1: Pouring temperatures used in the casting process of each alloy.

Sample ID	Pure Al	Al-1wt.%Zn	Al-10wt.%Zn	Al-30wt.%Zn	Al-60wt.%Zn
Temperature (°C)	730	730	720	690	640

Table 2: Alloy composition (wt.%) of the cast alloys in addition to aluminum determined according to ASTM E1097-12 and E1470-99(2011).

Alloy	Zn	Ti	B	Mg	Si	Cu	Mn	Fe	Cr
Pure Al	<0.01	0.10	0.010	<0.01	<0.01	<0.01	<0.01	<0.01	<0.01
1wt.%Zn	1.06	0.13	0.019	<0.01	<0.01	<0.01	<0.01	0.01	<0.01
10wt.%Zn	10.7	0.11	0.014	<0.01	0.02	<0.01	<0.01	0.07	0.01
30wt.%Zn	33.8	0.08	0.009	<0.01	0.04	<0.01	<0.01	0.08	<0.01
60wt.%Zn	62.2	0.05	0.007	<0.01	0.03	<0.01	<0.01	0.03	<0.01

2.2 Solutionizing and plane strain deformation

Samples with final dimensions of 57mm (l) x 12.7mm(w) x 8.2mm (t) were extracted from the casting, and individually re-solutionized at 428°C for 10 minutes in the salt bath and quenched into ice water. Within 5 minutes of quenching, reductions to 75% (2.4mm) and 90% (0.75mm) were started at 25°C using a channel-die for the pure aluminium, and a Stanat 2-high rolling mill for the other alloys. 75% and higher is beyond the texture transition issue in brass [7]. After the target reduction, half of the specimen was sectioned from the front end and put aside for characterization, with the remaining sample being further reduced. Note that the rolling deformation used approximately 5% reduction steps towards each target, while the channel die deformation was done continuously at a rate of 0.1mm/sec.

2.3 Texture and microstructure characterization

After deformation the specimens were mechanically ground using SiC papers, polished with diamond and colloidal silica to a center thickness on the RD-TD section, and electropolished using a by volume 70% ethanol – 20% distilled water – 8% perchloric acid – 2% butyl cellosolve solution at -20°C and 1.5 A/ cm² for 60 seconds. Four incomplete (111), (200), (220) and (311) pole figures were measured for each deformation condition using 50kV 190mA Cr-K α x-rays produced from a Rigaku DMAX rotating anode system with a 4-axis Huber cradle set-up with a Bragg-Brentano diffraction geometry. A vanadium filter was used in the measurement of the 10, 30 and 60%Zn alloys. Crystallographic orientation distribution functions were calculated from the pole figure data using the MTM-FHM analysis software to an LMAX of 22 [8]. All diffracted intensities were referenced to a random powder standard. Scanning electron microscopy imaging and orientation observations were made of select RD-ND sections using an FEI nano-SEM 450 equipped with Bruker e-FLASH detector.

3. Results

Figure 1 shows the incomplete $\{111\}$ pole figures measured for all the alloys at 75 and 90% reductions. From this data it is evident that the textures intensify with rolling reduction but weaken with alloying. Integrating all data, Fig. 2 plots the $\phi_2=90, 60$ and 45° sections for the same cases. Also shown for visual reference in overlay are some ideal texture components: cube, C $\{001\}\langle 100 \rangle$; goss, G $\{011\}\langle 100 \rangle$; brass, Br $\{011\}\langle 211 \rangle$; S $\{123\}\langle 634 \rangle$; and copper, Cu $\{112\}\langle 111 \rangle$.

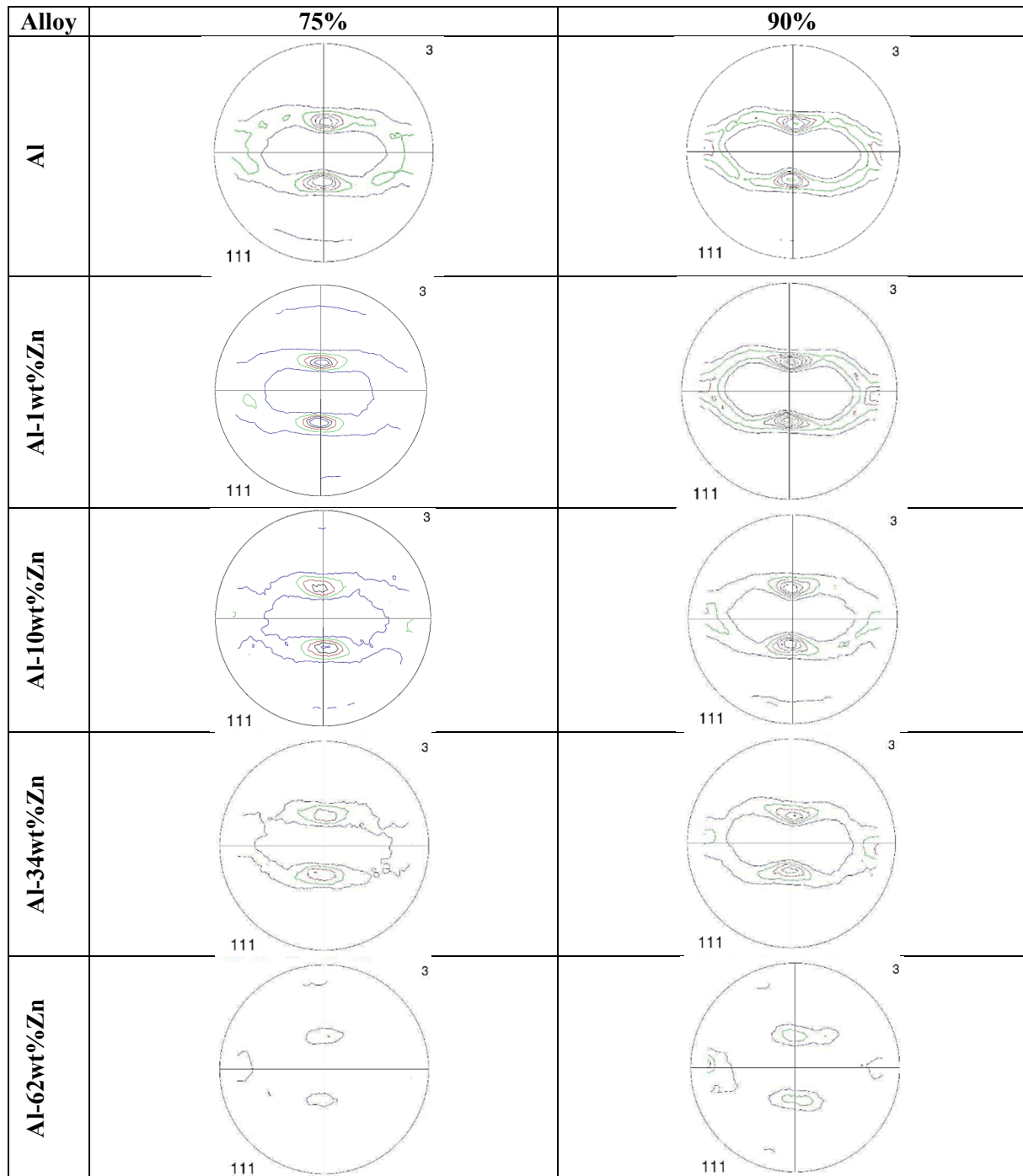


Fig. 1: As-measured incomplete $\{111\}$ pole figures for the Al-xZn alloys after 75 and 90% reductions in RD-TD sections of the center-plane. Contour lines are 1, 2, 3, 4, 5, 7.5 times random.

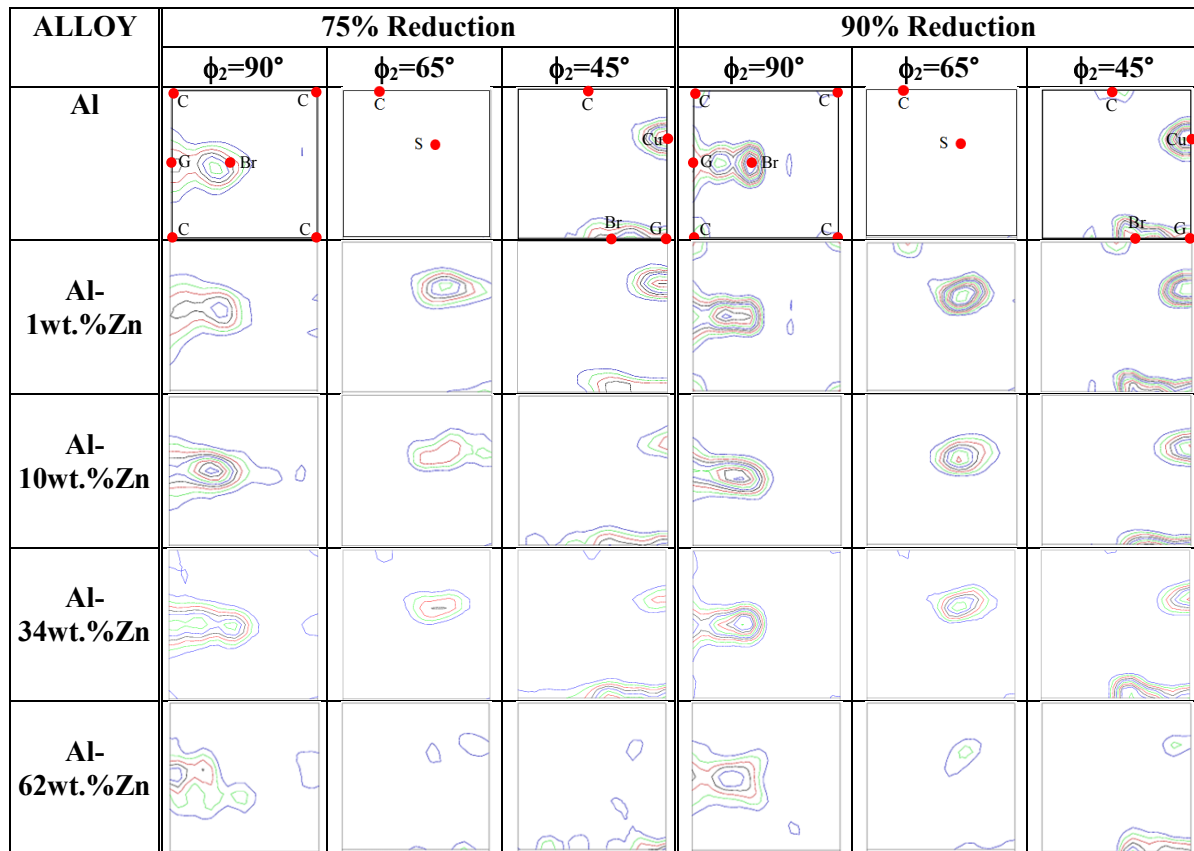


Fig. 2: CODF $\phi_2=90$, 65 and 45° sections for the same conditions as Fig. 1. Overlaid for comparison are ideal texture components cube (C), brass (Br), goss (G), copper (Cu) and S. Contour lines are 2, 3, 4, 5, 6, 7, 10, 12 times random.

4. Discussion

The rolling deformation of Al is similar yet quite different from the classic fcc textures of pure metal copper and the alloy brass, so that Al has its own texture characteristics. In the present work, plane strain deformation of pure Al from a random cast texture to 70 and 90% reductions results in the typical texture components of increasing Cu, Br and S components observed in many other rolling studies. Figure 3 shows the volume fractions of the main components in pure Al increase with deformation, but does not change for C and G. This trend for all the components remains in the Zn containing alloys.

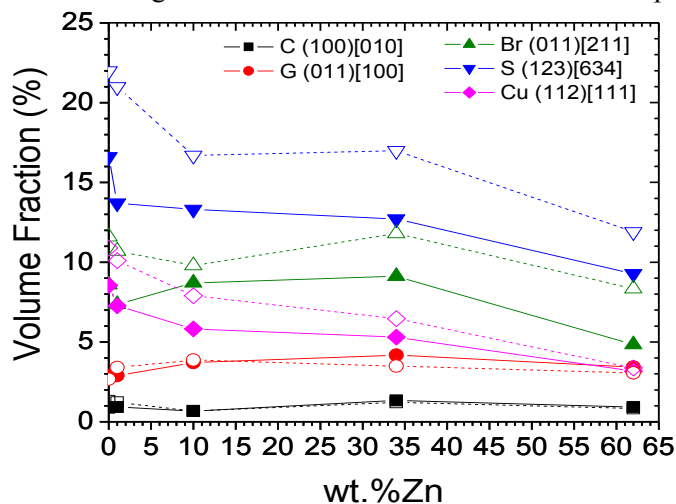


Fig. 3: Calculated volume fraction of select ideal texture components with Zn alloying and rolling reduction, where closed-symbols/solid lines are 70% and open-symbols/dashed lines are 90% reductions. The normalizing spread, Φ_0 , about the ideal orientation in Euler space is 11° .

Figure 3 also shows that alloying with Zn has some notable effects on the fraction of texture components. Firstly, C and G do not measurably change with alloying. Secondly, S, the largest component, and Cu decrease with Zn content. In contrast, Br decreases for 1%Zn, but then increases with alloying peaking at 12% for the Al-34wt.%Zn alloy rolled 90%. The S texture too shows a notable increase from 70 to 90% reduction. For the Al-62wt.%Zn alloy, all components decreased from the peak at 34wt.%Zn except the C and G, which did not change. The texture intensification at 90% reduction warranted a closer examination of the microstructure.

Figure 4 shows backscattered scanning electron images of the transverse sections of the Zn containing alloys after 90% reduction and sitting at room temperature for more than a year. All microstructures show lamellar banded structures aligned with the rolling direction with some particle decoration at the original boundaries. The pure Al microstructure (not shown) is very similar to the Al-1wt.%Zn. With alloying there is a greater propensity of heterogeneous deformation characterized by shear banding with rhombic-shaped bird's eye features prevalent in the 34 and 62wt.%Zn containing alloys. The eyes were more rounded, but less clear in the 60wt.%Zn alloy due to etching artefacts from the electropolishing of this reactive alloy.

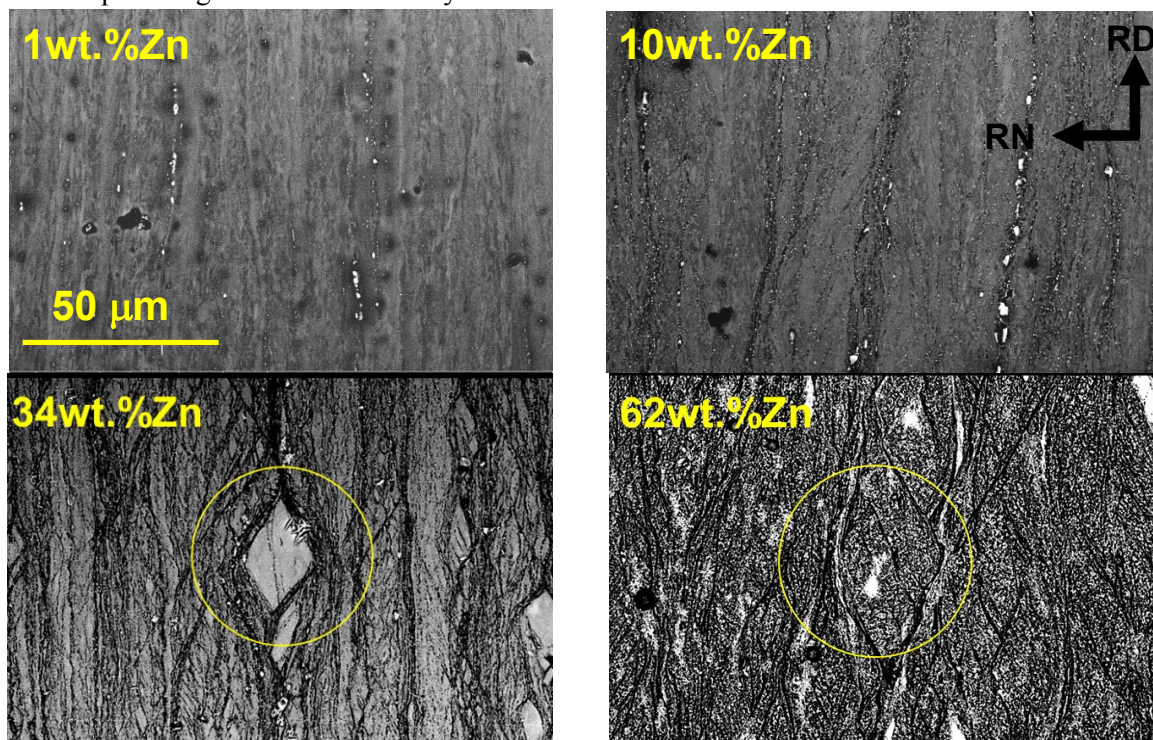


Fig. 4: Backscattered electron images of transverse sections of Al-xZn alloys after 90% reductions for (a) Al-1wt.%Zn, (b) Al-10%Zn, Al-34wt.%Zn and 62wt.%Zn. Circled regions show bird's eye features which are prevalent in the high Zn containing alloys. Imaging conditions were 10kV and 8mm WD using a CBS detector.

The orientation of the eye in the Al-34wt.% specimen is quite different from the surrounding orientations as indicated by the electron channelling effect of the backscattered image. The eye orientation was checked by electron backscattered diffraction, and the orientations plotted in $\{111\}$ and $\{220\}$ pole figures of Fig. 5. The feature is clearly a $\{110\}\langle 1-12 \rangle$ oriented grain and there is a splitting in the orientation data that matches an apparent slip band in the feature. The overall shape of the bird's eye is symmetric to the external strain coordinates and with an outline close to the $\{111\}$ slip intersections with the sectioning plane. Rhombic, lens-shaped domains have been reported for a range of rolled f.c.c. alloys since the 1970's: Cu-30Zn [10], Al-4.5Mg [11], and 316L stainless steel [12], but not for Al-xZn alloys to our knowledge. We will not speculate on the origin of the birds' eyes in this work except to

restate that it has a stable Br orientation and its presence is accompanied by surrounding slip and shear banding. Is the texture and microstructure development change with Zn a solid solution effect, or an effect of the deformation temperature? Even with a rapid quench the solid solution is unstable at 25°C for alloys with greater than 10wt.%Zn. At 298K, the T/T_m for the 30 and 60wt.%Zn alloys is greater than 0.35, which is the transition to non-octahedral slip [13]. The observed results are unlikely a stacking fault energy effect unless direct evidence of faults can be observed. See Leffers [14, 15] for a full review of the many nuances about the origin of the Br texture.

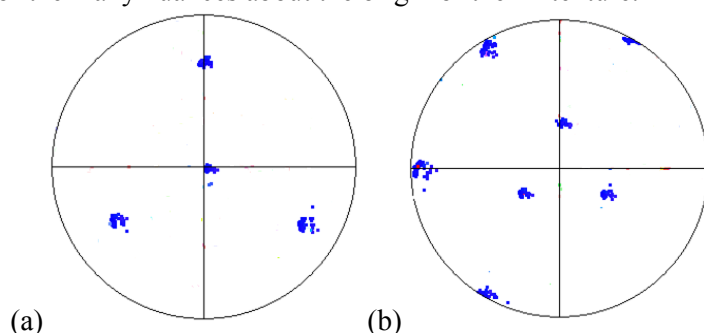


Fig. 5: (a) $\{111\}$ and (b) $\{220\}$ pole figures of bird's eye feature in Fig. 4(c) determined by electron backscattered diffraction. Vertical direction is the rolling direction and matches the orientation of the image in Fig. 4(c).

5. Conclusions

The evolution in rolling texture and microstructure of Al-xZn alloys after 70 and 90% reductions was studied. The Br-S-Cu intensity increased with rolling reduction, but increasing Zn weakened this effect except for some stabilization of Br. $\{110\}<1-12>$ microstructural “bird's eye” features were observed in 34 and 62wt.% Zn containing alloys at 90% reduction. No evidence for intrinsic stacking fault energy effects was observed, but the fundamental role of Zn in Al solid solution remains unclear and requires more detailed work hardening and microstructure-defect studies at higher reductions.

Acknowledgments

One of the authors (bjd) would like to thank M. Gallerneault for advice on using TiB₂ in casting the alloys, and acknowledges patient discussions with B. Hutchison, D.J. Lloyd and S. Saimoto about birds' eyes. The work was funded by an NSERC Discovery grant.

References

- [1] Hirsch J and Lücke K 1988 *Acta metall.* **36** 2863.
- [2] Douglass DL and Barbee TW 1969 *J. Matls. Sci.* **4** 121.
- [3] Douglass DL and Barbee TW 1969 *J. Matls. Sci.* **4** 138.
- [4] Hoyt JJ, Clark B, de Fontaine D, Simon JP, Lyon O 1989 *Acta metall.* **37** 1597.
- [5] Lloyd DJ, private communication, Dec. 2, 2015.
- [6] Karmakar G, Sen S, Chattopadhyay SK, Meikap AK, Chatterjee SK 2002 *Bull. Mater. Sci.* **25** 315.
- [7] Yeung WY, Hirsch J, Hatherley M 1988 *8th International Conference on Textures of Materials* (Santa Fe) (Warrendale: TMS) p 467.
- [8] Van Houtte P. MTM-FHM, Leuven, Belgium 2000.
- [9] Yeung WY, Hirsch J, Hatherley M 1988 *8th International Conference on Textures of Materials* (Santa Fe) (Warrendale: TMS) p 467.
- [10] Hutchinson WB, Duggan BJ, Hatherly M 1979 *Metals Tech.* Oct 398.
- [11] Lloyd DJ, Burtryn EF, Ryvola M 1982 *Microstructural Science* vol. 10 (Elsevier) p 373.
- [12] Donadille C, Valle R, Dervin P, Penelle R 1989 *Acta metall.* **37** 1547.
- [13] Cortez-Regalado H and Saimoto S 1984 *7th International Conference on Textures and Materials* (Noordwijkerhout) (Netherlands: The Netherlands Society for Materials Science) p 39.
- [14] Leffers T 1996 *11th International Conference on Textures and Materials* (Beijing) vol. 1 (Beijing: Intl. Academic Publishers) p 299.
- [15] Leffers T, Ray RK 2009 *Prog. Matls. Sci.* **54** 351.